II International Conference on Particle-based Methods – Fundamentals and Applications
PARTICLES 2011
E. Oñate and D.R.J. Owen (Eds)

NUMERICAL MODEL BASED ON MESHLESS METHOD TO SIMULATE FSW

A.TIMESLI[1, 2], H.ZAHROUNI[1], B.BRAIKAT[2], A.MOUFKI[1], H.LAHMAM[2]

[1] Université Paul Verlaine de Metz, Laboratoire d'Etude des Microstructures et de Mécanique des Matériaux, LEM3, UMR CNRS 7239, Ile du Saulcy 57045, Metz Cedex 01 France.
[2] Université Hassan II Mohammedia - Casablanca, Faculté des Sciences Ben M'sik, Laboratoire de Calcul Scientifique en Mécanique, Casablanca, Maroc.

Key words: FSW, Simulation, Meshless, SPH

Abstract. In the present work, a numerical models based on the meshless method "the smoothed particle hydrodynamics (SPH)" is developed to simulate the Friction Stir Welding (FSW). This technique type is well adapted to modeling of mixing zone which is subjected to high strain rate. We limit ourselves to two dimensional problems.

1. INTRODUCTION

Friction Stir Welding (FSW) was invented by the British Welding Institute TWI since 1990s for aluminum sheets [1]. The main advantage of this technique is its ability to joining in solid state a class of metal alloys which are generally difficult to weld by conventional welding processes. Joining two workpieces by FSW consists in heat generation due mainly to the shoulder and material mixing thanks to the pin. Heat is generated two main mechanisms, friction and plastic dissipation [2-4].

Numerical modeling of FSW has been investigated by several authors considering thermal or thermo-mechanical framework. Different formulations have been proposed in these contributions concerning Eulerian, Lagrangian or Arbitrary Lagrangian Eulerian formulations [5-9]. The choice of a specific formulation is mainly oriented by the relevant phenomenon that authors have to analyze. In the face of the numerous industrial applications of FSW process, its development remains largely empirical and based on and based on a large experimental knowledge of the process. Experimental works are very numerous. The numerical simulations also but the treatment of mixing remains a major difficulty for the numerical analyst. The numerical modeling of FSW has been investigated by several authors considering thermal or thermomechanical framework. Different formulations have been proposed in these contributions concerning Eulerian, Lagrangian or Arbitrary Lagrangian Eulerian formulations. The choice of a specific formulation is mainly oriented by the relevant phenomenon that authors have to analyze. The mixing is difficult to achieve using the finite element method because the area near the welding tool is the seat of large deformations. For this, we propose in this work using the meshless methods.

In this work, a numerical model based on the smoothed particle hydrodynamics SPH [10-14]

method is developed to simulate the Friction Stir Welding. This model considers a non Newtonian fluid near the tool region using a thermomechanical constitutive law.

The main advantage of this technique concerns that the material mixing around the tool which is very difficult or impossible to achieve with other numerical methods such as finite element method. The history of the particles is available; one can obtain the residual stresses.

For plates of large sizes, the mixing zone rest very localized. This is the area where the strains are very large and generate a source of intense heat. Entire plate contributes to heat exchange with the outside environment. One idea is to treat the localized area near the tool so different from the rest of the plate. We propose in this work using a technique based on meshless method to model the mixing of material around the tool.

2. SPH MODEL FOR 2D SIMULATION OF FRICTION STIR WELDING

2.1. GOVERNING EQUATIONS

The different equations needed to simulate the Friction Stir Welding process by SPH are given by the conservation laws including:
First, the mass conservation:

$$\frac{d\rho}{dt} = -\rho \nabla . v \tag{36}$$

The second equation describes the classical momentum conservation:

$$\frac{dv}{dt} = \frac{1}{\rho} \nabla \sigma \tag{37}$$

The third equation is energy conservation:

$$\rho c_p \frac{\partial T}{\partial t} = \nabla . (k \nabla T) + q_v \tag{38}$$

The rate of heat generation due to plastic deformation is given by:

$$q_v = -\beta (\tau : \nabla v) \tag{39}$$

where β represent the fraction of mechanical energy transformed to heat and is assumed to be 0.9 [15].
The stress tensor is given by:

$$\sigma = -pI + \tau \tag{40}$$

Where p is the hydrostatic pressure, I the identity tensor and τ the deviatoric stress tensor:

$$\tau = \mu [\nabla v + (\nabla v)^T - \frac{2}{3} (\nabla . v) I] \tag{41}$$

Viscosity of the particles decreases with increasing temperature according to:

$$\mu = A \left(1 - \left(\frac{T - T_{ref}}{T_{melt} - T_{ref}} \right)^m \right) \tag{42}$$

A and m are material parameters. T_{ref} is a reference temperature and T_{melt} is the melting temperature. The pressure is obtained using the equation of state:

$$P = c^2 \rho \tag{43}$$

c is the speed of sound.

2.2. PRINCIPLE OF SPH METHOD

The SPH method is based on an integral approximation [11]:

$$f(\vec{r}) = \int f(\vec{r}')\, W(\vec{r} - \vec{r}', h)\, d\vec{r}' \tag{44}$$

Where h is the smoothing length and W is the kernel function. The approximate forms of the integral by SPH:

$$f(\vec{r}_a) = \sum_{b=1}^{Np} \frac{m_a}{\rho_b} f_b W\left(\left\|\vec{r}_a - \vec{r}_b\right\|, h\right) \tag{45}$$

$$\nabla f(\vec{r}_a) = \sum_{b=1}^{Np} \frac{m_a}{\rho_b} (f_a - f_b) W\left(\left\|\vec{r}_a - \vec{r}_b\right\|, h\right) \tag{46}$$

Where m_b, ρ_b et N_p are the mass, the density of the particle b et the number of neighboring particles respectively. Example: kernel function type cubic spline [16]:

$$W(\|\vec{r}_a - \vec{r}_b\| r, h) = \alpha_d \times \begin{cases} 1 - \frac{3}{2} q^2 + \frac{3}{4} q^3 & \text{si } q \le 1 \\ \frac{1}{4}(2-q)^3 & \text{si } 1 \le q \le 2 \\ 0 & \text{si } q \ge 2 \end{cases} \tag{47}$$

With $q = \dfrac{\left\|\vec{r}_a - \vec{r}'_b\right\|}{h}$

And $\alpha_d = \begin{cases} 10/(7\pi h^2) & en\ 2D \\ 1/(\pi h^3) & \text{en } 3D \end{cases}$

2.3. SPH FORMULATION AND TIME DISCRETIZATION

Using SPH approximations of functions and its spatial derivatives the governing equations are discretized resulting in a set of ordinary differential equations:

$$\frac{d\rho_a}{dt} = \sum_{b=1}^{Np} m_b \vec{v}_{ab} \vec{\nabla}_a W_{ab} \tag{48}$$

$$\frac{d\vec{v}_a}{dt} = -\sum_{b=1}^{Np} m_b \left(\frac{P_b}{\rho_b^2} + \frac{P_a}{\rho_a^2} + \Pi_{ab} \right) \vec{\nabla}_a W_{ab} + \sum_b \frac{4 m_b \mu_a \mu_b}{\rho_a \rho_b (\mu_a + \mu_b)} \frac{(\vec{v}_a - \vec{v}_b).(\vec{r}_a - \vec{r}_b)}{(\vec{r}_a - \vec{r}_b)^2} \vec{\nabla}_a W_{ab} \tag{49}$$

$$C_{p,a}\left(\frac{dT}{dt}\right)_a = \sum_b \frac{m_b}{\rho_a \rho_b} \frac{4 k_a k_b}{(k_a + k_b)} (T_a - T_b) \frac{(\vec{r}_a - \vec{r}_b).\nabla W(r_a - r_b, h)}{(\vec{r}_a - \vec{r}_b)^2} + q_v - h(T_a - T_{ref}) \tag{50}$$

$$q_v = \beta \sum_b \frac{2m_b \mu_a \mu_b}{\rho_a \rho_b (\mu_a + \mu_b)} \frac{[(\vec{v}_a - \vec{v}_b).(\vec{r}_a - \vec{r}_b)]^2 (\vec{r}_a - \vec{r}_b)}{(\vec{r}_a - \vec{r}_b)^2} \vec{\nabla}_a W_{ab} \tag{51}$$

$$\mu_a = A\left(1 - \left(\frac{T_a - T_{réf}}{T_{melt} - T_{ref}}\right)^m\right) \tag{52}$$

$$p_a = c^2 \rho_a \tag{53}$$

2.3.1. BOUNDARY CONDITIONS

To avoid penetration of the particles representing weld material into the tool, boundary particles are forced to satisfy the same equations as fluid particles. Thus, they follow the momentum equation, the continuity equation, the equation of state, and the energy equation. However, they do not move according to the XSPH variant. They move together with velocities:

$$\vec{v}_i = \vec{r}_{i,c}\omega + \vec{v}_t, \vec{r}_{i,c} = (x_i - x_c, z_i - z_c, 0), \tag{54}$$

Where ω is the rotational velocity and v_t is the translational velocity of the tool. x_c and z_c are coordinates of the tool rotation axis. When a fluid particle approaches a boundary the density of the boundary particles increases according to the continuity equation (Eq. 48) resulting the increasing pressure following the equation of state (Eq. 53). Thus, the force applied on the fluid particle increases due to the pressure term (P/ρ^2) in momentum equation (Eq. 49). When the distance between the boundary particle and the fluid particle becomes smaller than 2h, the density, pressure and force applied on the incoming particle increase generating the repulsion mechanism.

2.3.2. TIME DISCRETIZATION SCHEME

The time scheme to deal with the derivatives in time is the explicit "velocity Verlet" algorithm [17] as follows:

$$\begin{aligned} &\vec{v}_a^{n+1} = \vec{v}_a^n + 0.5\Delta t(\vec{F}_a^n + \vec{\mathrm{F}}_\mathrm{a}^{\mathrm{n+1}}) \;;\; \rho_a^{n+1} = \rho_a^n + 0.5\Delta t(D_a^n + \mathrm{D}_\mathrm{a}^{\mathrm{n+1}}) \\ &\vec{r}_a^{n+1} = \vec{r}_a^n + \Delta t\vec{V}_a^n + 0.5\Delta t^2\vec{F}_a^n \;;\; T_a^{n+1} = T_a^n + 0.5\Delta t(E_a^n + \mathrm{E}_\mathrm{a}^{\mathrm{n+1}}) \end{aligned} \tag{55}$$

With $\frac{d\vec{v}_a}{dt} = \vec{F}_a, \frac{d\rho_a}{dt} = D_a, \frac{d\vec{r}_a}{dt} = \vec{V}_a, \frac{dT_a}{dt} = E_a$

2.4. NUMERICAL DISCUSSION

We consider a plate made of aluminum alloy with L=50 mm length and a width of 20 mm (see Figure 4). The parameters of the law (Eq. 52) are defined as follows: A = 200 Mpa.s^{-1}, m=1, T_{ref} = 25°C, T_{melt} = 502°C.

The tool is rigid and made of steel material with cylindrical geometry (r_p=2.5 mm rayon). The physical properties (material conductivity k, specific heat C_p, and density ρ) used for aluminum plate are presented on table 1.

ρ (kg/m3)	Cp (J/K.kg)	k (W/m.K)
2780	875	140

Tableau 1: Physical proprieties

In the proposed work, we have used a heat transfer coefficient h_{lat}=30 W/m^2.K, a ambient temperature T0=25°C, a welding velocity of 2 mm/s and a rotation speed of 20 rad/s.

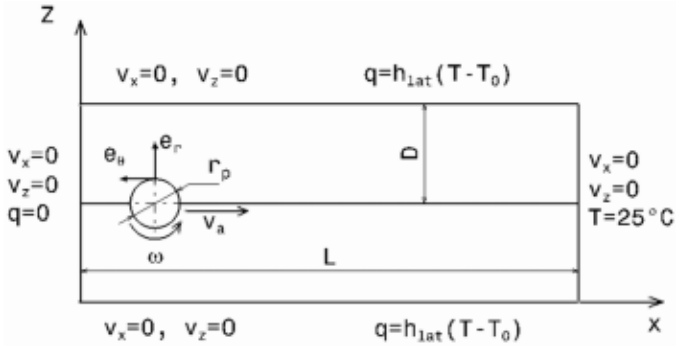

Figure 4: Geometry and boundary conditions of FSW configuration treated by SPH

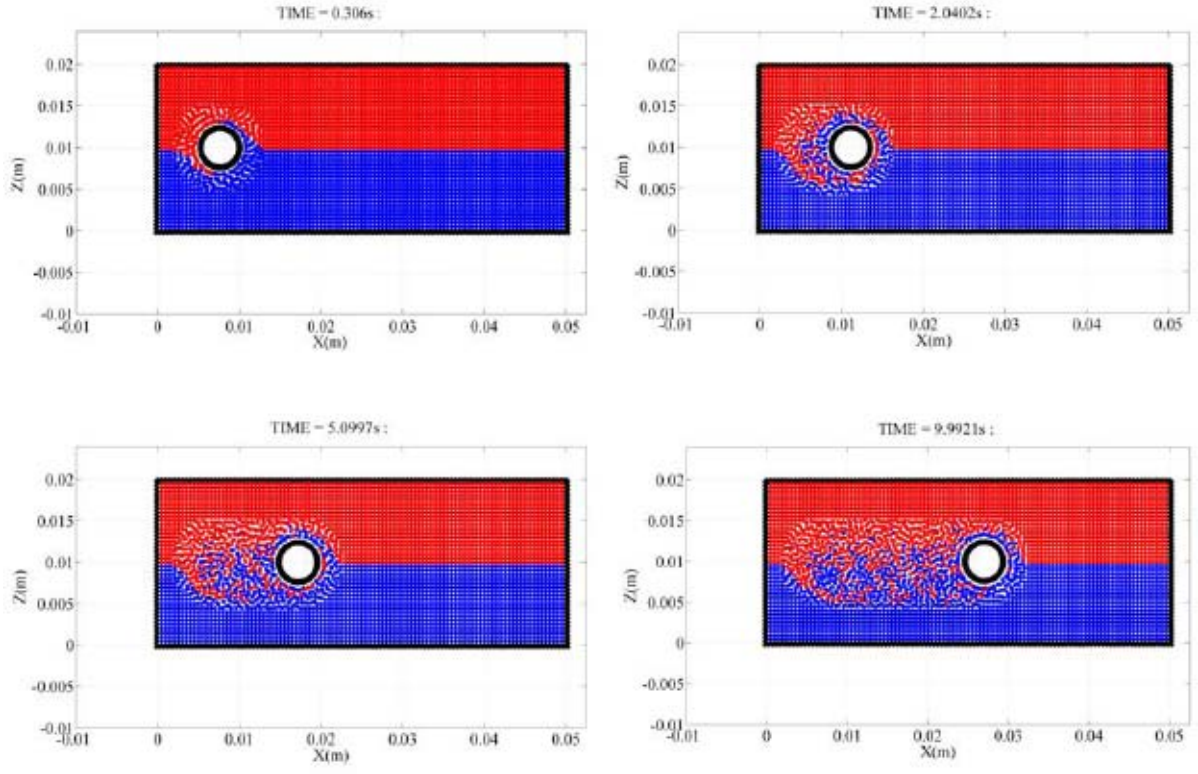

Figure 5: Mixing of particles around the welding tool by SPH

Figure 5 presents the figures of mixing of material for different computing time; these figures represent the positions of discrete dots of material. This result shows the advantage of the SPH method to simulate industrial processes involving large deformation such as FSW process. The distribution of the temperature field is shown in Figure 6.

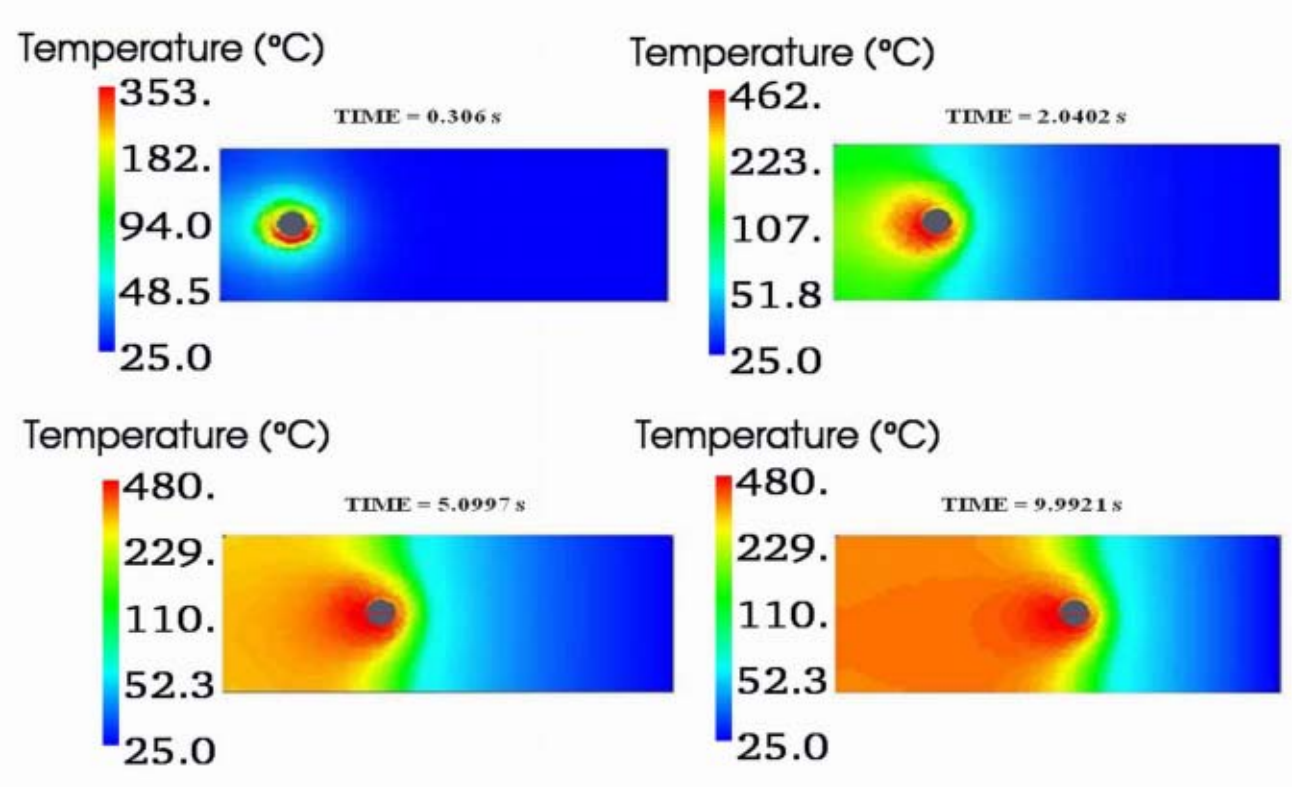

Figure 6: Temperature distribution equivalent to the mixing of configurations of figure 2

The results of our approach are compared with those obtained using the Fluent software. This code is based on an Eulerian formulation and a finite volume discretization. To validate the results of our algorithm, we choose two equivalent configurations between the two formulations Lagrangian and Eulerian (Figure 4 and 7). The SPH calculation is performed until the tool reaches the plate center. This computation needs a time t = tc = 9s. In the eulerian formulation, unsteady calculation with a time tc is performed (Figure 8). The two calculations use the same constitutive law (Eq. 52). Figure 10 and 11 shows the comparison between SPH and Fluent of temperature evolution along the horizontal and vertical section (see Figure 9) using kernel function type Gaussian. One can observe that a relative error of at least 2% is obtained confirming the relevance of the proposed algorithm.

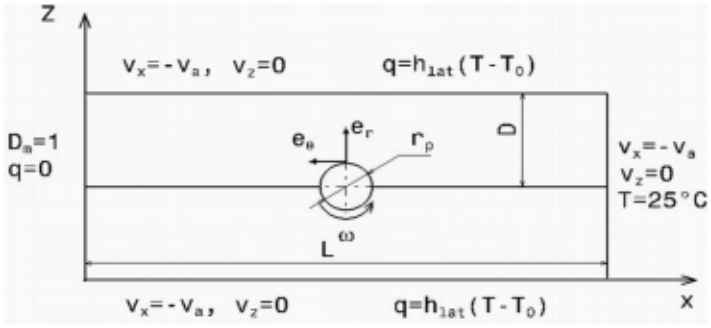

Figure 7: Geometry and boundary conditions of FSW configuration treated by Fluent

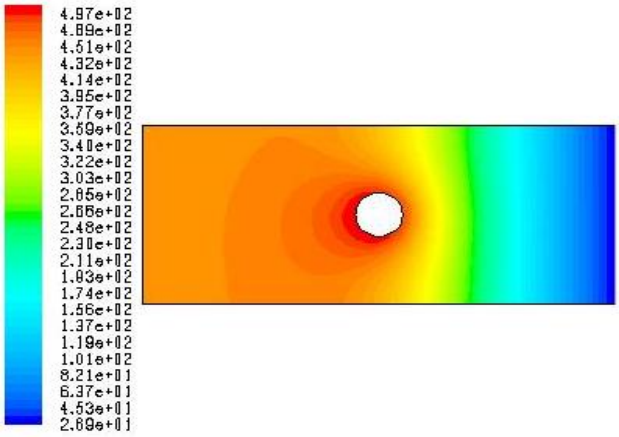

Figure 8: Temperature distribution by Fluent

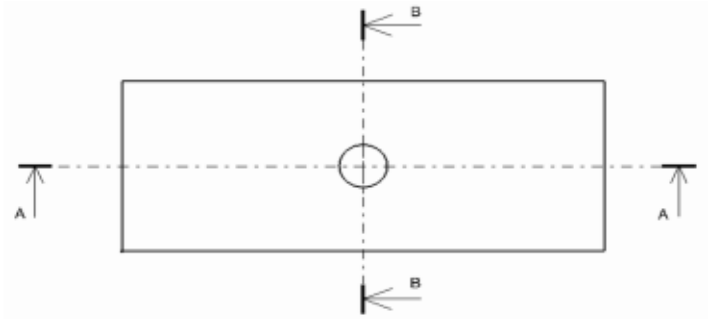

Figure 9: Horizontal section (A-A) and vertical section (B-B)

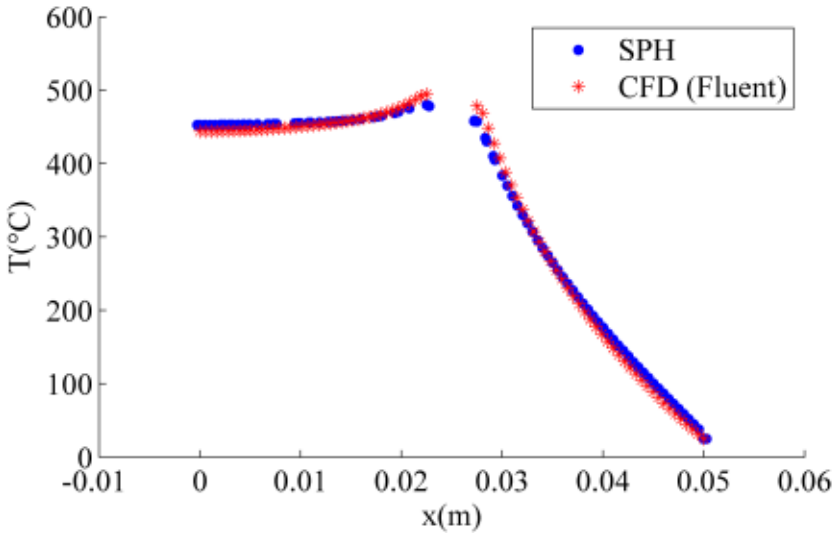

Figure 10: Temperature evolution along the horizontal section (A-A): kernel function type Gaussian

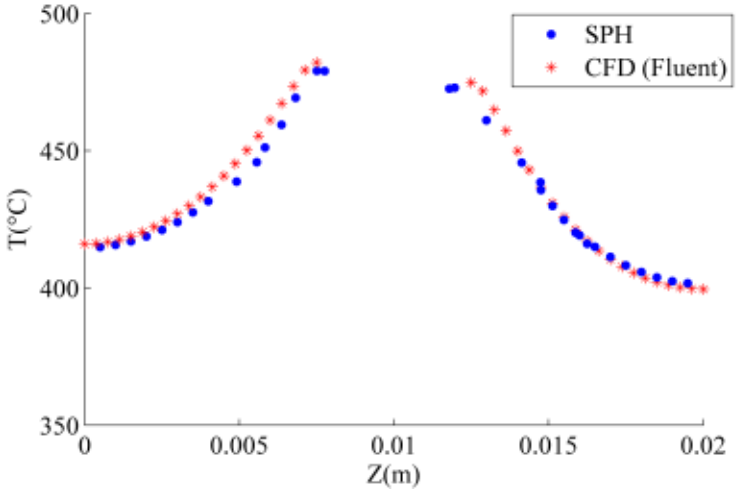

Figure 11: Temperature evolution along the vertical section (B-B): kernel function type Gaussian

2.5. FSW SIMULATION

In the following, and after validation of the model, we propose a more realistic constitutive law. Furthermore, we propose a model coupling that will allow the simulation of welding of large plates. A local model that will simulate the mixing around the welding tool is coupled to a thermal model that takes into account the entire structure and its environment. It does not take much time because the search of neighbors is done once only for the thermal model

2.5.1. CONSTITUTIVE LAW

The constitutive relation is chosen in this form:

$$\mu(T,\bar{\dot{\varepsilon}}) = \frac{\bar{\sigma}}{3\bar{\dot{\varepsilon}}} \tag{22}$$

Where $\bar{\dot{\varepsilon}}$ is the equivalent strain rate, and $\bar{\sigma}$ is the von Mises equivalent stress given by:

$$\bar{\sigma} = \frac{1}{\alpha}\sinh^{-1}\left(\frac{Z(\bar{\dot{\varepsilon}},\mathrm{T})}{A}\right)^{\frac{1}{n}} \tag{23}$$

Which $Z(\bar{\dot{\varepsilon}},\mathrm{T})$ represents the Zener-Hollomon parameter:

$$Z(\bar{\dot{\varepsilon}},\mathrm{T}) = \bar{\dot{\varepsilon}}\exp\left(\frac{\mathrm{Q}}{\mathrm{RT}}\right) \tag{24}$$

Where Q is the activation energy, R the gaz constant, and n are material parameters given in reference [18].

2.5.2. RESULTS

We consider a plate made of aluminum alloy (aluminum 6061) with 90 mm length and a width of 60 mm. The mechanical and thermal characteristics are given in the following table:

ρ (kg/m3)	Cp (J/K.kg)	k (W/m.K)
2780	980	140

Tableau 2: mechanical and thermal characteristics

In the present work, we use a heat transfer coefficient hlat=17 W/m^2.K, a ambient temperature T0=25°C, a welding velocity of 2 mm/s and a rotation speed of 20 rad/s.

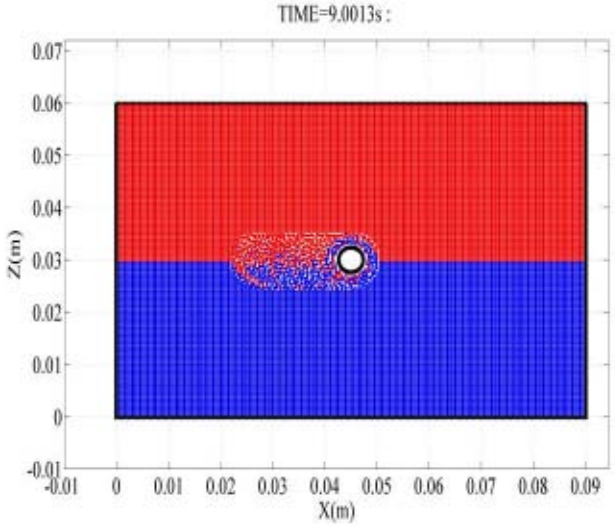

Figure 12: Mixing of particles

Figure 12 present the mixing of material at t = 9s; this figure represent the positions of discrete dots of material. The distribution of the temperature field is presented in Figure 13.

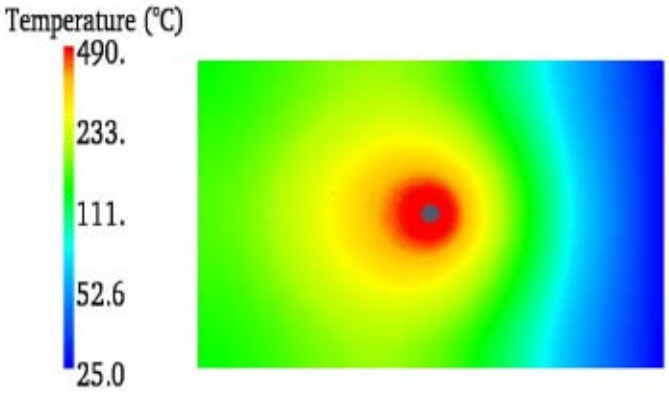

Figure 13: Temperature distribution

Figure 14 and 15 shows the temperature evolution along the horizontal and vertical section (see Figure 9) using kernel function type Gaussian.

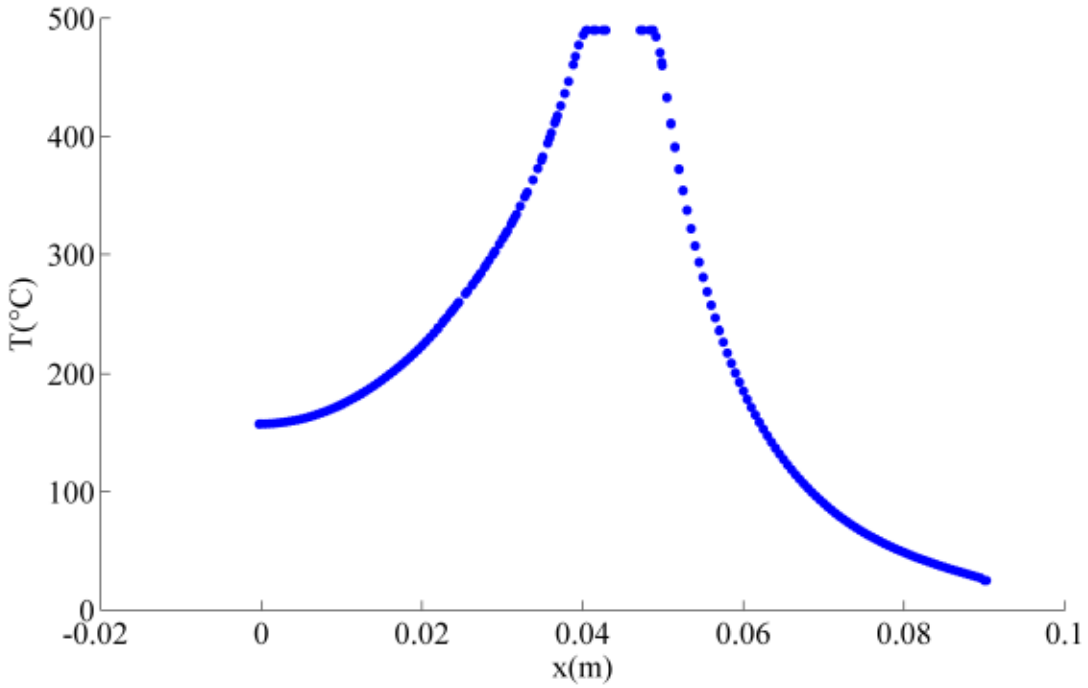

Figure 14: Temperature evolution along the horizontal section (A-A)

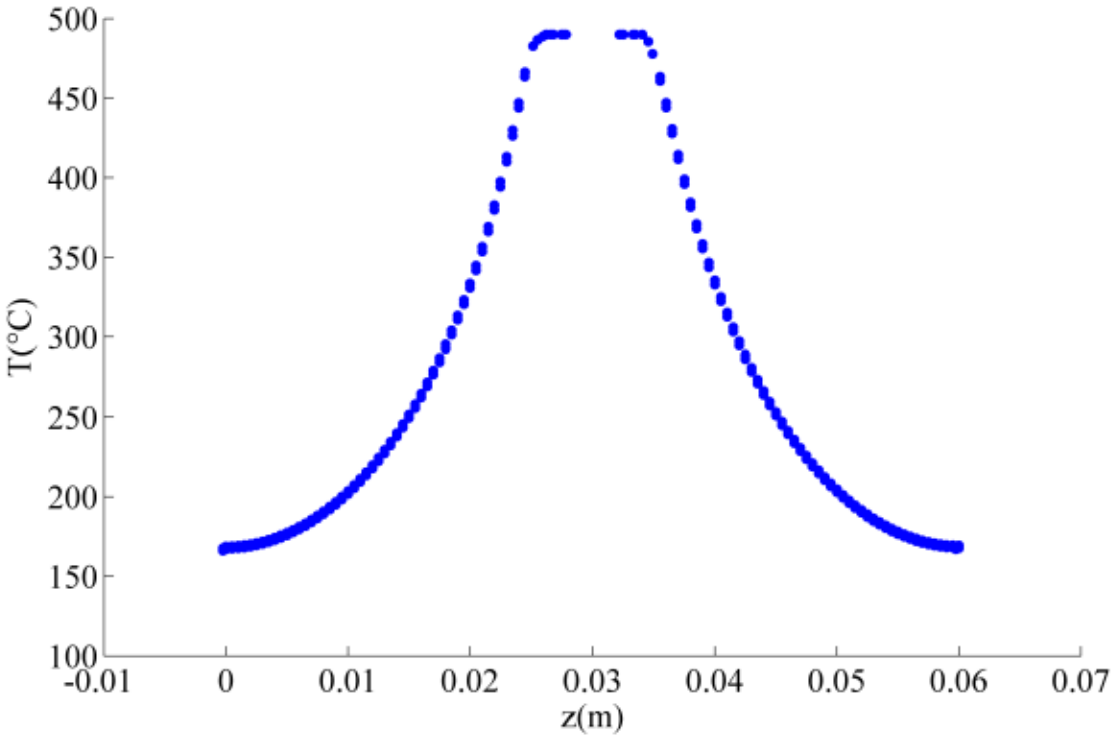

Figure 15: Temperature evolution along the horizontal section (B-B)

3. CONCLUSION

Material mixing is very difficult or impossible to achieve with other numerical methods such as finite element method because material zone located near the welding tool is subjected to high strain gradient and remeshing procedure is often necessary.

In this contribution, we have proposed a first model based on SPH to model FSW process. The main advantage of this technique concerns that the material mixing around the tool. The history of the particles is available; one can obtain the residual stresses.

REFERENCES

[1] W. M. Thomas, E. D. Nicholas, J. C. Needham, M. G. Church, P. Templesmith and C. Dawes, Intl. Patent Application no. PCT/GB92/02203 and GB Patent Application no. 9125978.9, 1991.
[2] K. Colligan, "Material Flow Behavior during Friction Stir Welding of Aluminium", Welding Journal, vol. 78(71), 229-237, 1999.
[3] T. U. Seidel and A. P. Reynolds, Science and Technology of Welding and Joining, vol. 8, 175-183, 2003.
[4] T. U. Seidel and A. P. Reynolds, "Visualization of the Material Flow in AA2195 Friction-Stir Welds Using a Marker Insert Technique", Metallurgical and Materials Transaction, vol. 32, 2879-2884, 2001.
[5] H. Schmidt, J. Hattel. "Thermal modelling of friction stir welding". Scripta Materialia, vol. 58, 332–337, 2008.
[6] O. Lorrain, J. Serri, V. Favier, H. Zahrouni, M. El Hadrouz, "A contribution to a critical review of FSW numerical simulation" , J. Mec. Mat. Str., Vol. 4, 351-369, 2009.

[7] A. Bastier, M.H. Maitournam, F. Roger, K. Dang Van, " Modelling of the residual state of friction stir welded plates", Journal of Materials Processing Technology, Volume 200, Issues 1-3, Pages 25-37, 8 May 2008.
[8] S. Guerdoux, L. Fourment, "A 3D numerical simulation of different phases of friction stir welding", Modell. Simul. Mater. Sci. Eng. 17 (2009)
[9] E. Feulvarch, Y. Gooroochur, F. Boitout, J.M. Bergheau, "3D Modelling of Thermofluid Flow in Friction Stir Welding", TRENDS IN WELDING RESEARCH, PROCEEDINGS, Pages 261-266, 2006.
[10] J.J.Monaghan, "An introduction to SPH", Comput. Phys. Commun. 48 (1) (1988) 89-96.
[11] J.J. Monaghan, Smoothed Particle Hydrodynamics, Annu. Rev. Astrophys. 30: pp. 543-574, 1992.
[12] J.J. Monaghan, J. Comput. Phys. 82 (1989) 1.
[13] G. R. Liu, M. B. Liu, Smoothed Particle Hydrodynamics - A Meshfree Particle Method, World Scientific Publishing Co. Pte. Ltd. 5 Toh Tuck Link, Singapore 596224.
[14] A. M Tartakovsky, G. Grant, X. Sun and M. Khaleel, Modeling of Friction Stir Welding (FSW) Process with Smooth Particle Hydrodynamics (SPH) , SAE 2006 World Congress, Detroit, USA, 2006.
[15] J. Zhou, L. Li, and J. Duszczyk. 3D FEM simulation of the whole cycle of aluminium extrusion throughout the transient state and the steady state using the updated Lagrangian approach. Journal of Materials Processing Technology, 134:383-397, 2003.
[16] G. R. Liu, M. B. Liu, Smoothed Particle Hydrodynamics - A Meshfree Particle Method, World Scientific Publishing Co. Pte. Ltd. 5 Toh Tuck Link, Singapore 596224.
[17] M.P. Allen and D.J. Tildesley, Computer simulation of liquids (Oxford University Press, Oxford,) p.81, 2001.
[18] D.H. Lammlein, D.R. DeLapp, P.A. Fleming, A.M. Strauss, G.E. Cook. "The application of shoulderless conical tools in friction stir welding: An experimental and theoretical study". Materials and Design, vol 30, 4012–4022, 2009.